Supporting Information

Modification of the Poly(bisdodecylquaterthiophene) (PQT12) Structure for High and Predominantly Nonionic Conductivity with Matched Dopants

Hui Li,[†] Mallory E. DeCoster,[‡] Robert M. Ireland,[†] Jian Song,[†] Patrick E. Hopkins[‡] and Howard E. Katz[*,†]

[†]Department of Materials Science and Engineering, Johns Hopkins University, 3400 North Charles Street, Baltimore, Maryland 21218, USA

[‡]Department of Mechanical and Aerospace Engineering, University of Virginia, Charlottesville, Virginia 22904, USA

[*]E-mail: hekatz@jhu.edu

Contents

Materials and Methods: All chemical reagents and starting materials were purchased and used without further purification, unless otherwise noted. ^{1}H NMR (400 MHz) spectra of monomers were recorded on Bruker Avance spectrometer using $CDCl_3$ as solvent and tetramethylsilane (TMS) as the internal standard. ^{1}H NMR spectra of PDTDE12 and PDTDES12 were conducted using toluene-d_8 as solvent at 100 ^{o}C. Molecular weights were determined using gel permeation chromatography on a Waters 1515 Isocratic HPLC with a Waters 2489 UV/vis detector using polystyrene as standard and THF as eluent. UV-vis-NIR absorption spectra were taken on Agilent Cary 5000 spectrophotometer. The absorption intensity was normalized by the film thickness. Cyclic voltammetry (CV) was performed in a one-chamber, three-electrode cell in dry acetonitrile containing 0.1 M *n*-Bu_4NPF_6 as a supporting electrolyte. A glass carbon disk, a platinum wire and Ag/AgCl electrode, were used as the working electrode, auxiliary electrode and reference electrode, respectively. A ferrocene/ferrocenium redox couple as an external standard, whose oxidation potential is set at -4.8 eV with respect to zero vacuum level. Geometries optimization was performed at the level of B3LYP /6-31G by using Gaussian09. UPS was conducted with He I radiation ($h\nu$ = 21.2 eV) of a helium discharge lamp and the samples were prepared by drop casting the solution on the glass substrate with 50 nm Au deposited on top first. AFM images were taken in tapping mode using a Dimensional 3100 AFM (Bruker Nano, Santa Barbara, CA). The images were visualized using the Nanoscope software (Bruker). GIXRS measurements were performed at the Advanced Photon Source (APS), Argonne National Laboratory using x-rays with a

wavelength of λ = 1.6868 Å. The samples were prepared by drop casting the solution onto silicon wafer substrates, and then annealed in the nitrogen at 120 ^{o}C for 10 min. The thickness of films was measured by KEYENCE VK-X100 Laser microscope with 3D & profile measurement.

OFET Fabrication and Characterization: Top contact/bottom gate OFET devices were fabricated using highly n doped Si/SiO_2 substrates. The substrates were cleaned and modified with hexamethyldisilazane (HMDS) self-assembled monolayer. The polymers were dissolved in chlorobenzene with the concentration of 5 mg mL^{-1}. The thin films were prepared by spin coating the solution on the substrates. Then the polymer thin-film was annealed on a hot plate at 120 °C for 10 min under N_2 atmosphere. Gold contacts of 50 nm were deposited on the thin film as source and drain electrodes with a channel width of 8000 µm and a channel length of 250 µm. The electrical performance of transistors was carried out using an Agilent 4155C Semiconductor Parameter analyzer in ambient. The mobility was calculated in the saturation regime according to the equation: $I_{DS} = (W/2L)\mu C_i(V_G - V_T)^2$, where I_{DS} is the drain current, μ is the mobility, and V_G and V_T are the gate voltage and threshold voltage, respectively.

Thermoelectric Device Fabrication and Characterization: Glass substrates (Corning Inc.) were cleaned by sonication in deionized water, acetone and *i*-propanol. Gold electrodes (50 nm thick) were deposited on glass with a channel length of 3 mm and a channel width of 7 mm. Polymer and dopant were dissolved in chlorobenzene

separately with the concentration of 5 mg mL^{-1}. The polymer and the dopant solution were heated and sonicated at 70 ºC for 30 min. Then the polymer was blended with dopant in the desired concentration. The mixture solution was heated at 50 ºC and sonicated for 30 min. The final solution was dropped on the glass substrate on which 2D wells are fabricated by laying a pattern of Novec polymer. After evaporation of solvent, a square film forms. The devices were annealed on a hot plate at 120 ºC for 10 min in nitrogen. All the measurements were performed in ambient. Resistance was measured by using four-probe measurement method with an Agilent 4155C Semiconductor Parameter Analyzer. At least three measurements of resistance were performed on each sample surface in different positions. Seebeck coefficient can be calculated by $S=\Delta V/\Delta T$, where ΔV is the thermal voltage obtained between the two electrodes of the device subjected to a temperature gradient ΔT. Six ΔT were imposed on the sample, so the slopes of ΔV versus ΔT give values of the Seebeck coefficient.

The Calculation of Carrier Concentration: Take 1 gram sample of 40 wt %F4TCNQ doped PDTDE12 as example (molar ratio = 1.1). There is 0.71 g polymer and 0.29 g F4TCNQ in this solid. If all repeat units of polymer are assumed to be doped, the number of the repeat units of polymer equals the number of the carrier. Carrier number = 0.71 g/781 g mol^{-1} = 9.1×10^{-4} mol. The density of sample is assumed to be 1 g cm^{-3}, therefore, the carrier concentration = 9.1×10^{-4} mol × 6.02×10^{23} mol^{-1} cm^{-3} = 5.5×10^{20} cm^{-3} (all percentages mentioned in paper are dopant in polymer).

Thermal Conductivity Measurements: The thermal conductivities of PDTDE12 and PDTDES12 each doped with 20% F4TCNQ, as well as PQT12 and PQTS12 each doped with 10% NOBF4 were measured using time domain thermoreflectance (TDTR).[1,2] The PDTDE12 and PDTDES12 polymers were drop casted onto the aluminum side of a SiO_2/Al substrate, consisting of 80 nm of Al which had been electron-beam evaporated onto the bulk SiO_2. The PQT12 and PQTS12 polymer films were prepared slightly differently due to significant degredation of the Al layer which occured during the polymer deposition process. Therefore, these polymers were drop casted onto the gold side of a SiO_2/Au substrate. This substrate consisted of 68 nm of Au which had been electron-beam evaporated directly onto a bulk SiO_2 slide, with no adhesion layer. The 80 nm of Al and 68 nm of Au serves as transducers to convert the optical energy provided by the TDTR laser pulse, to thermal energy into the sample. The temporal decay of this event is measured, and provides information about the intrinsic thermal properties of the sample. The thermal decay curves for PDTDE12 and PQTS12 along with their corresponding heat conduction models are shown in Figure S12.

TDTR is a non-contact optical thermometry technique with a pump-probe configuration. A sub-picosecond oscillator provides ~100 fs pulses at a repetition rate of 80 MHz centered at a wavelength of 800 nm (FWHM = 10.5 nm). This output is split into two paths, a pump path and a probe path. The pump and probe spot sizes are focused down to $1/e^2$ radii of 12 μm and 7 μm, respectively. The pump beam is electronically modulated at a frequency of 10 MHz with a square wave. The pump

beam passes through the transparent SiO_2 substrate and heats the metallic transducer layer, creating a bi-directional modulated heating event (into the SiO_2 substrate and into the polymer film). The reflectivity of the metallic transducer (Al or Au) changes linearly with the polymer surface temperature, and is monitored temporally by the probe beam. The probe beam is mechanically delayed in time between 500 ps up to 6 ns, and its reflected intensity is measured by a balanced photodetector. Further, a lock-in amplifier demodulates and signal and provides amplidue and phase data in the form of a thermal decay curve. A heat conduction model is fit to these thermal decay curves in order to determine relevent thermal properties of the material.[2-4] In these TDTR measurements, since we are probing through the SiO_2 substrate, a bi-directional heat model is considered in the analysis.[5] We also determine that our TDTR signal is sensitive to the effusivity of both the SiO_2 and the polymer. This means that our TDTR signal is equally sensitive to thermal conducitivity and volumetric heat capacities of each material; therefore to measure one parameter (i.e. thermal conductivity), the other must be known. It should also be noted here that due to this sensitivity regime, uncertainties in the assumed heat capacity propogate to uncertainties in the the measured thermal conducitivities. We assume literature values for the heat capacities of the Al, Au and SiO_2, along with literature values for the thermal conuctivity of the evapoated Al and Au thin films.[3] The thermal conductivity of the SiO_2 substrate was measured with TDTR before the polymer was deposited (κ = 1.38 +/- 0.04 W m^{-1} K^{-1}). Since the heat capacities of the doped PDTDE12, PDTDES12, PQT12, and PQTS12 polymer films have not been reported, we assume

a heat capacity of that for P3HT, since the chemical structure of their backbones is similar, and propogate 20% uncertainty about this assumed heat capacity into our error analysis.[6] The total uncertainity encompassed by our error bars associated with the thermal conductivity measurements are further characterized by a 3 nm uncertainty in the transducer film thickness. Additionally, we measure the electical resistivities of the Al and Au transducer layers with a home-built four point probe technique. From these measured electrical resistivities, we calculate the electrical component to the thermal conductivity of the films using the Wiedemann-Franz law and input the respective values for the thermal conducitivty of the Au or Al in our three layer heat model (κ_{Au} = 228 +/- 5.0 W m^{-1} K^{-1} and (κ_{Al} = 140 +/- 13 W m^{-1} K^{-1}).

The Calculation of HOMO Energy Level of polymers: Ferrocene/ferrocenium (Fc/Fc^+) was used as external reference. The redox potential of Fc/Fc^+ was assumed to have an absolute energy level of -4.80 eV to vacuum. The redox potential of Fc/Fc^+ was measured under the same conditions, and it is located at 0.16 V to the Ag/AgCl electrode. The energy levels of the highest occupied molecular orbital (HOMO) was calculated according to the equations: HOMO = -e(E_{ox} + 4.64) (eV), where E_{ox} is the onset oxidation potential vs Ag/AgCl.

The Calculation of LUMO Energy Level of NOBF4: We calculated the LUMO level of NOBF4 according to the redox potential of nitrosonium (NO^+) which is 1.27~1.25 V vs SCE (saturated calomel electrode).[7,8] Based on -4.4 ~ -4.7 eV SCE energy level

relative to vacuum,[9,10] LUMO = - e(E_{red} + 4.5) (eV). The LUMO level of 5.7 eV in Figure 1 is an average value.

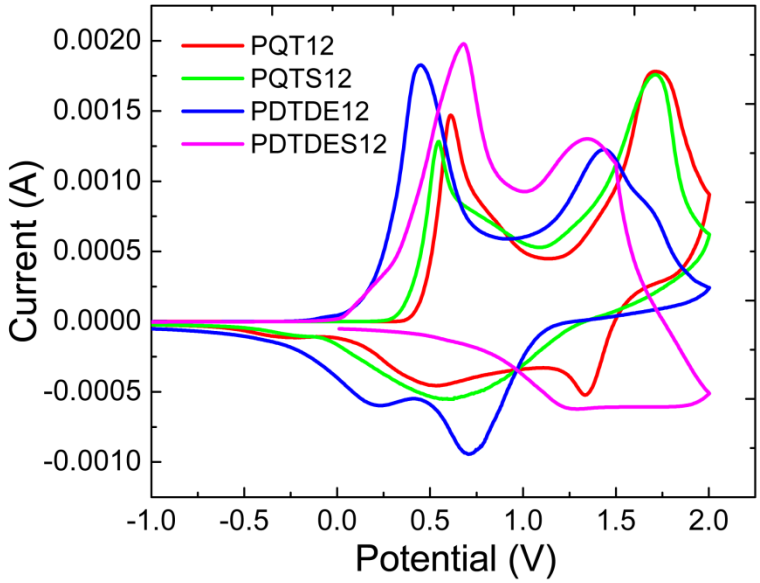

Figure S1. Cyclic voltammograms of PQT12, PQTS12, PDTDE12 and PDTDES12 films.

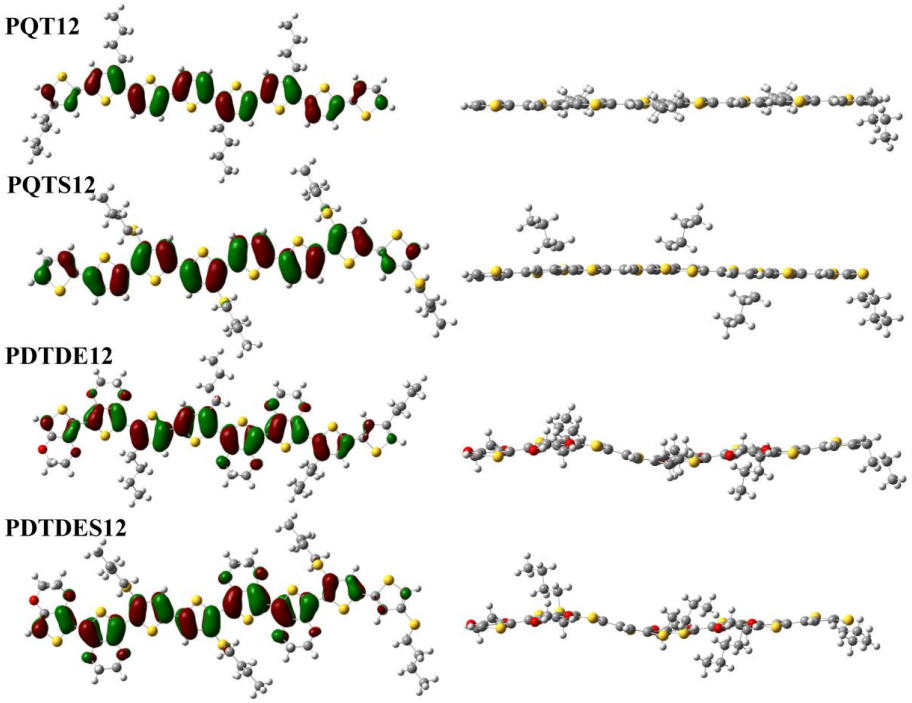

Figure S2. Calculated HOMO (left) and the optimized configuration (right) of the dimers of four polymers (B3LYP/6-31G). Long alkyl chains are replaced with butyl groups to simplify calculation.

Table S1. The integrated area of polaronic absorption and neutral absorption and the ratios between two bands for doped polymers.

polymer/dopant	A_I (700 ~ 1200 nm)	A_{II} (400 ~ 700 nm)	A_I/A_{II}
PQT12/NOBF4	74.5	76.9	0.97
PQTS12/NOBF4	89.2	74.2	1.20
PQT12/F4TCNQ	34.0	65.2	0.52
PQTS12/F4TCNQ	37.5	60.5	0.62
PDTDE12/NOBF4	94.4	52.8	1.79
PDTDES12/NOBF4	94.4	42.0	2.25
PDTDE12/F4TCNQ	128.3	84.3	1.52
PDTDES12/F4TCNQ	44.7	36.3	1.23

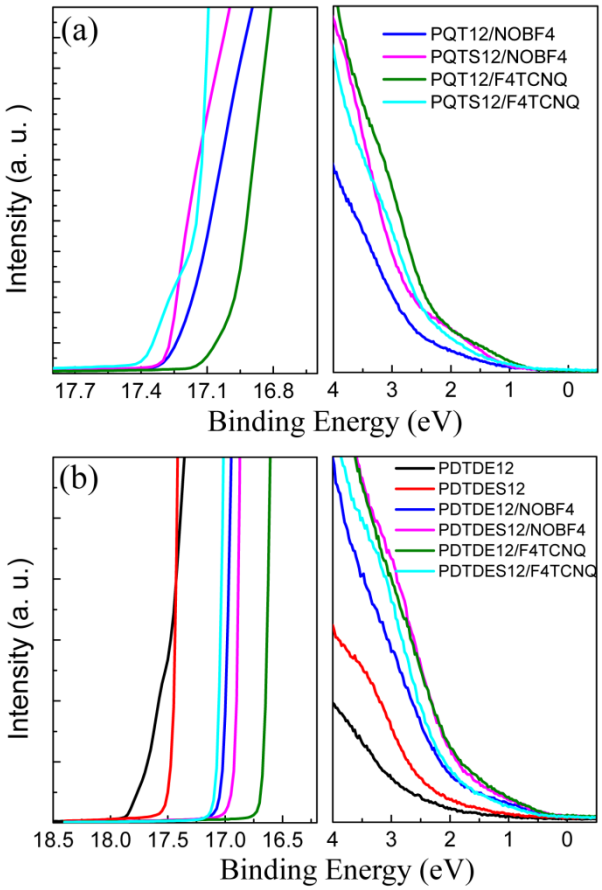

Figure S3. UPS spectra of doped PQT12 and PQTS12 (a) and pure PDTDE12, PDTDES12 and doped PDTDE12 and PDTDES12 (b). Work function region (left) and valence region (right). All binding energies are reported relative to the E_F.

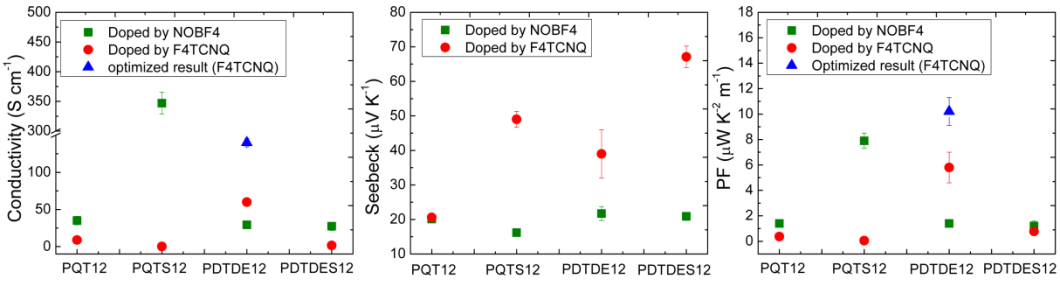

Figure S4. Thermoelectric parameters of all polymers doped by NOBF4 and F4TCNQ.

Table S2. Thermoelectric properties of doped polymers with molar ratio of 0.5 (the data in bracket are the optimized values by changing the molar ratio).

polymer/dopant	σ (S cm^{-1})	S (μV K^{-1})	PF (μW m^{-1} K^{-2})	λ (W m^{-1} K^{-1})	ZT
PQT12/NOBF4	35.0±5.7	20.1±1.1	1.4±0.3	0.405±0.109	1.03×10^{-3}
PQTS12/NOBF4	347±18.2	16.2±0.98	7.9±0.6	0.461±0.159	5.11×10^{-3}
PQT12/F4TCNQ	8.8±0.5	20.6±0.7	0.37±0.1	—	—
PQTS12/F4TCNQ	0.8±0.05	49.0±2.3	0.05±0.006	—	—
PDTDE12/NOBF4	29.3±1.2	21.7±2.0	1.4±0.3	—	—
PDTDES12/NOBF4	27.3±5.6	20.9±1.2	1.2±0.4	—	—
PDTDE12/F4TCNQ	60.0±5.4 (140.1)	39.0±7.0	5.8±1.2 (11.0)	0.232	0.014
PDTDES12/F4TCNQ	1.6±0.4 (4.2)	67.1±3.1	0.78±0.12	0.282±0.058	8.24×10^{-4}

Table S3. Crystallographic parameters calculated from GIXRS profiles for PQT12, PQTS12 and doped films (the value in round brackets is from the scattering of neutral F4TCNQ; the value in square brackets represents the increase compared with pure polymer).

Sample	Out of plane		In plane	
	q_z (Å^{-1})	lamellar distance (Å)	q_{xy} (Å^{-1})	π-π stacking (Å)
PQT12	0.35	18.2	1.56	4.00
PQTS12	0.32	19.6	1.69	3.70
PQT12/NOBF4	0.32	19.9 [1.7]	1.74	3.61
PQTS12/NOBF4	0.27	22.9 [3.3]	1.78	3.53
PQT12/F4TCNQ	0.32	19.9 [1.7]	1.75	3.57
PQTS12/F4TCNQ	0.31	20.4 [0.8]	1.74 (0.81)	3.61

Table S4. Crystallographic parameters calculated from GIXRD profiles for PDTDE12, PDTDES12 and doped films (the value in round brackets is from the lamellar structure; the value in square brackets represents the increase compared with pure polymer).

Sample	Out of plane		In plane	
	q_z (Å^{-1})	lamellar distance (Å)	q_{xy} (Å^{-1})	π-π stacking (Å)
PDTDE12	0.30	20.9	—	—
PDTDES12	0.35	18.5	1.67 (0.67)	3.77 (18.7)
PDTDE12/NOBF4	0.27	22.9 [2.0]	1.77	3.55
PDTDES12/NOBF4	0.28	22.5 [4.0]	1.76	3.56
PDTDE12/F4TCNQ	0.30	20.7 [-0.2]	1.74	3.61
PDTDES12/F4TCNQ	0.30	20.7 [2.2]	(0.28)	(22.4)

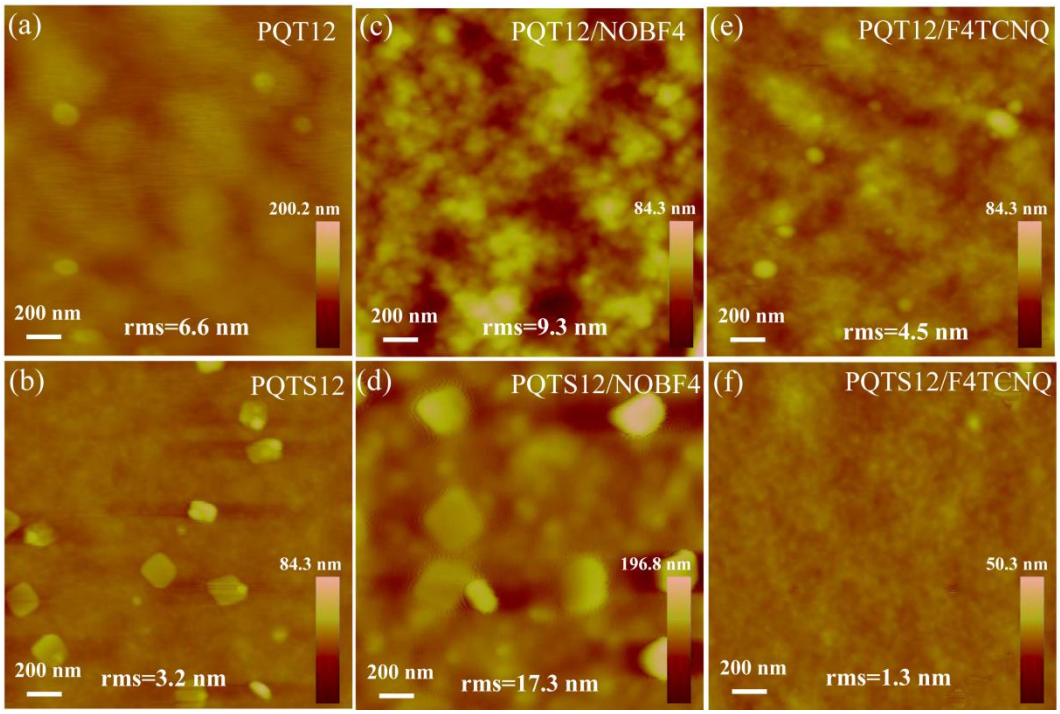

Figure S5. AFM height images of pure PQT12, PQTS12 and corresponding doped films. Films were prepared as the same procedure for thermoelectric measurements.

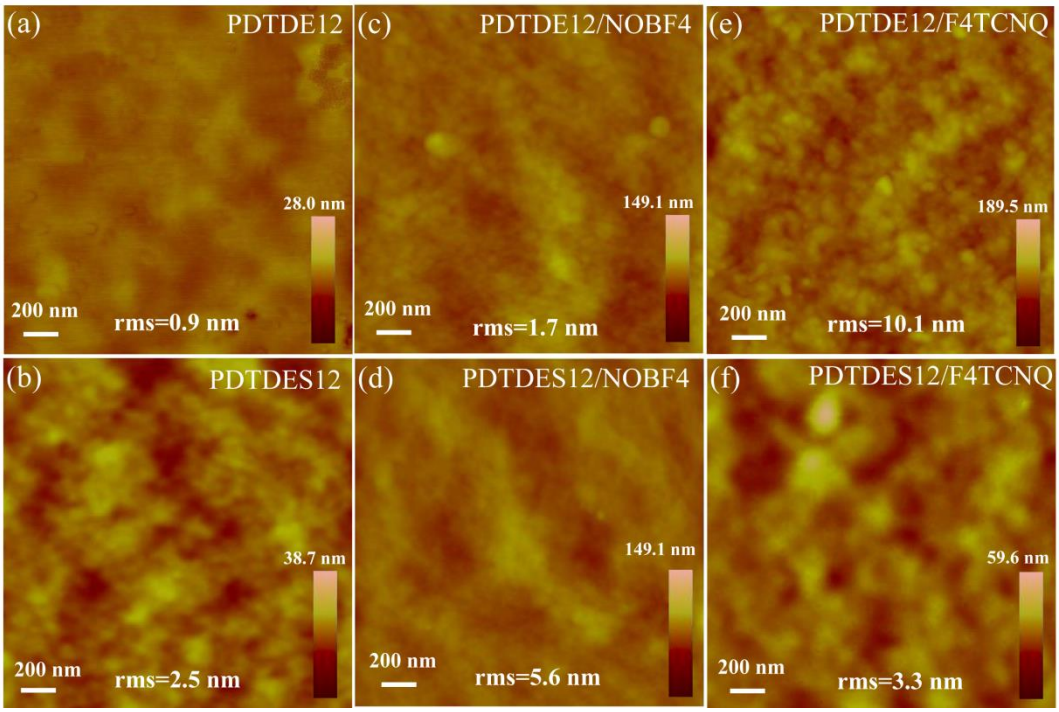

Figure S6. AFM height images of pure PDTDE12, PDTDES12 and corresponding doped films. Films were prepared as the same procedure for thermoelectric measurements.

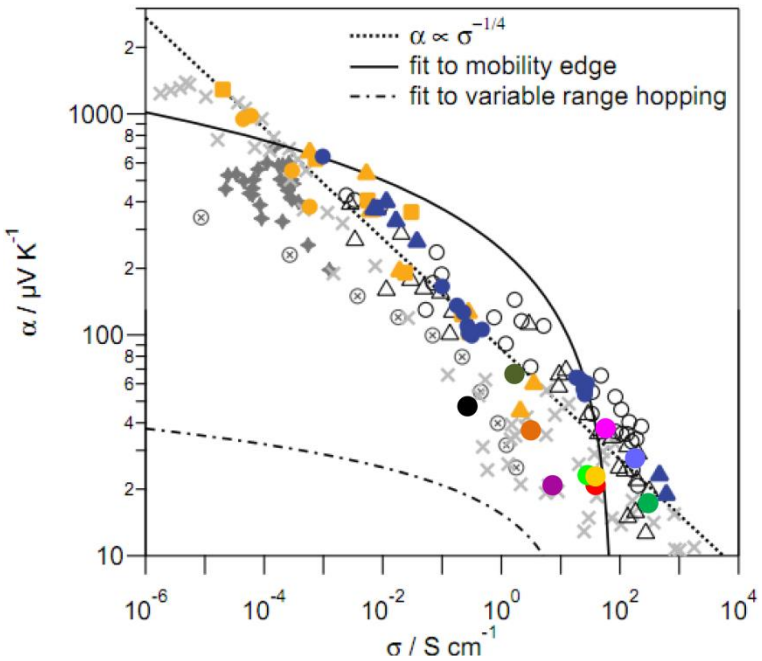

Figure S7. Fits of relationship between Seebeck and conductivity of doped polymers in Table S3 using the Chabinyc empirical model of Reference 23, copyright John Wiley and Sons, used with permission.

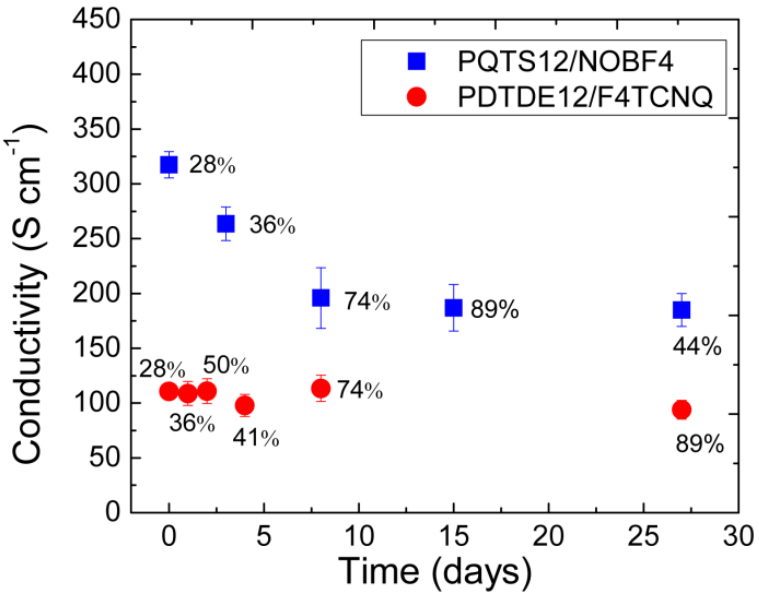

Figure S8. Long term air-stability measurements of optimal devices of PQTS12/NOBF4 and PDTDE12/F4TCNQ under different humidity (the value next to the point is the humidity during measurement). The devices were stored in a transparent plastic box without any further actions to exclude the exposure of light or humidity.

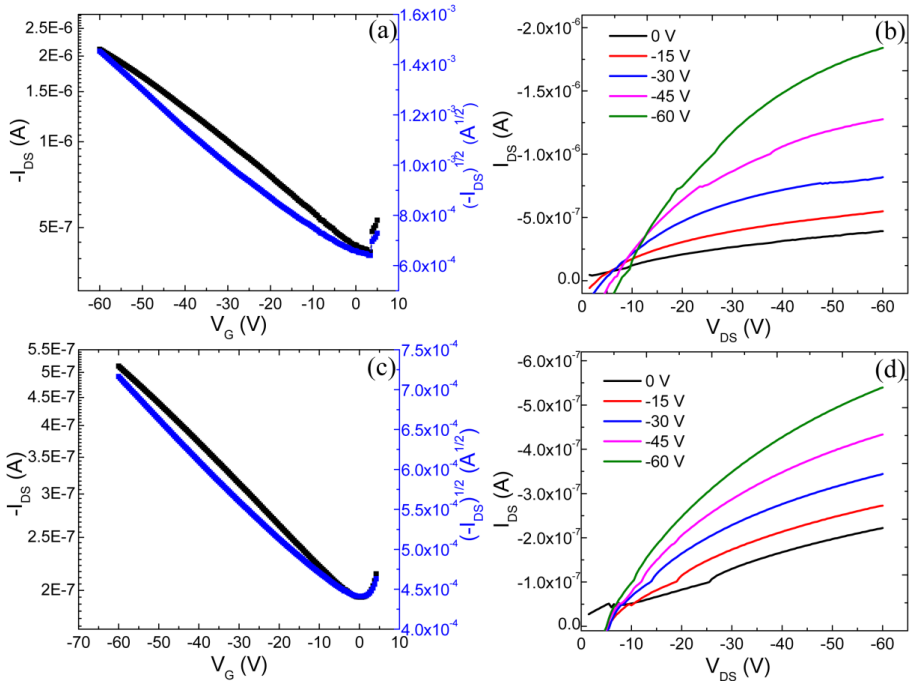

Figure S9. The transfer (V_{DS} = -60 V) and output curves of PDTDE12 (a, b) and PDTDES12 (c, d) based OFET devices annealed at 120 °C for 10 min.

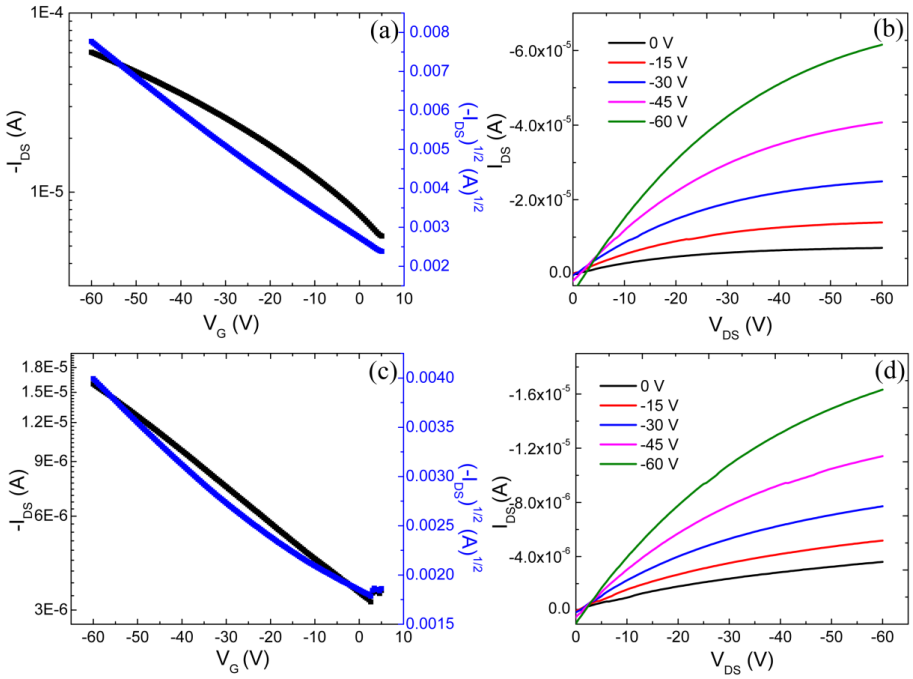

Figure S10. The transfer (V_{DS} = -60 V) and output curves of 3% NOBF4 doped PQTS12 (a, b) and 0.5 wt % F4TCNQ doped PDTDE12 (c, d) based OFET devices annealed at 120 ^{o}C for 10 min.

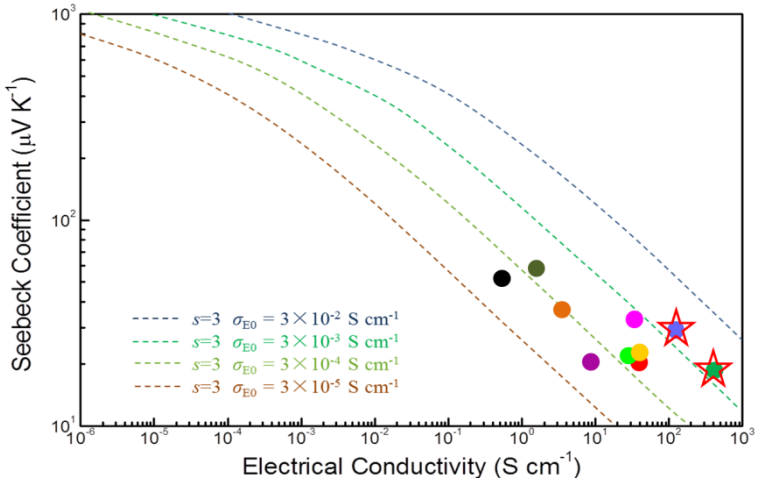

Figure S11. The Seebeck coefficiency versus electrical conductivity relation (data from Table S3) using Snyder's model in Reference 15 (removing data points of original figure).

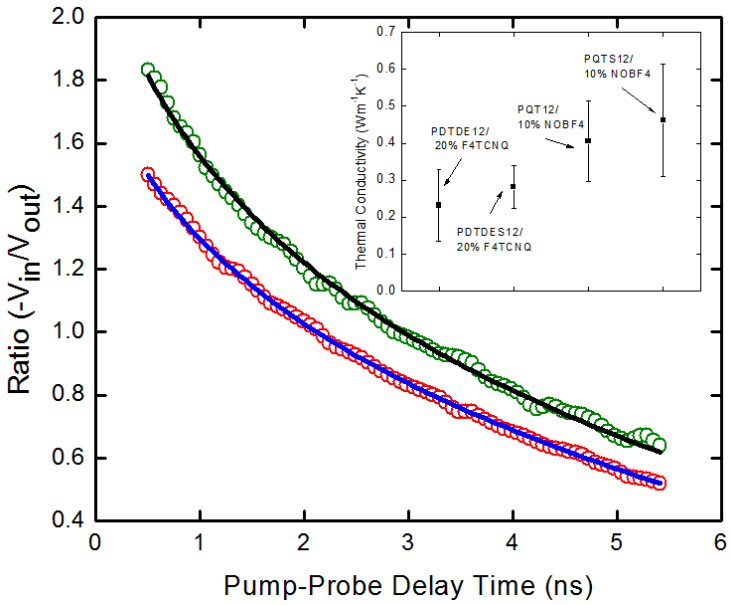

Figure S12. Representative TDTR data (thermal decay curve) of PDTDE12 (red circles with the corresponding heat conduction model shown as the blue line) and PQTS12 (green circles and the corresponding heat conduction model shown as the black line). From the fit of the models (line) we can determine the thermal conductivity of each polymer (shown in the subset).

Table S5. Summary of thermoelectric properties of the previously reported p-doped conjugated polymers and the results in this work.

Materials	σ (S cm^{-1})	S (μV K^{-1})	PF (W m^{-1} K^{-2})	λ (W m^{-1}K^{-1})	ZT	Processing method	Ref.
PEDOT:PSS -DMSO	890	74	470	0.24	0.42	doped during synthesis and spin cast	11
PEDOT-Tos	90	780	324	0.37	0.25	doped during synthesis and spin cast	12
Polycarbazole /$FeCl_3$	160	34	19	—	—	immersing film in dopant solution	13
P3HT /ferrictriflimide	80	50	20	—	—	immersing film in dopant solution	14
PBTTT/NOPF6	55	13	0.98	—	—	immersing film in dopant solution	15
PBTTT14 /F4TCNQ	248	—	—	—	—	evaporate the dopant on top of a PBTTT14 layer	16
PBTTT14/FTS	604	19	22	—	—	vapor-deposition, measured under nitrogen	17
PBTTT14/FTS	1000	33	110	—	—	vapor-deposition, measured under nitrogen	18
PBTTT14 /F4TCNQ	3.5	60	1.3	—	—	solution casting, measured under nitrogen	19
P3HT/F4TCNQ	1.8	—	—	—	—	spin-cast from solution	20
p(g42T-T) /F4TCNQ	100	11	1.2	—	—	spin coating or drop casting	21
PDPP(6-DO)$_2$TT /CN6-CP	70	—	—	—	—	drop casting	22
PDPP(6-DO)$_2$TT /F6TCNNQ	2	—	—	—	—	drop casting	23
PQTS12 /NOBF4	350	15	8	0.461±0.159	0.0051	drop casting	this work
PDTDE12 /F4TCNQ	140	22	11	0.232±0.098	0.014	drop casting	this work

Abbreviations: PEDOT=poly(3,4-ethylenedioxythiophene), PSS=polystyrene sulfonate, P3HT=poly(3-hexylthiophene), PBTTT=poly(2,5-bis(3-tetradecylthiophen-2-yl)thieno[3,2-b]thiophene), PDPP(6-DO)$_2$TT=poly[3,6-(dithiophene-2-yl)-2,5-di(6-dode -cyloctadecyl)-pyrrolo[3,4-c]pyrrole-1,4-dione-alt-thieno[3,2-b]thiophene], FTS= (tridecafluoro-1,1,2,2-tetrahydrooctyl)trichlorosilane.

Synthetic Procedure and Characterization

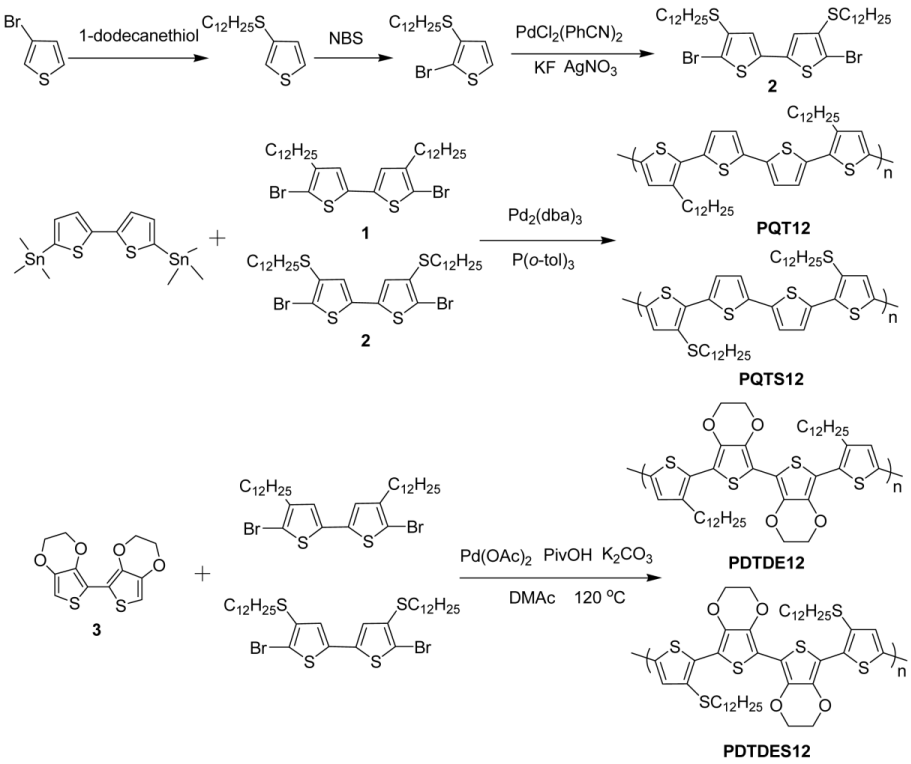

Figure S13. The synthetic routes to the four polymers.

Monomer **1** was synthesized from 2-bromo-3-dodecylthiophene following a literature procedure.[24] A solution of 2-bromo-3-dodecylthiophene (1 g, 3.0 mmol) and DMSO (50 ml) was stirred at room temperature. 3 mol% of $PdCl_2(PhCN)_2$ (34.7 mg, 0.09 mmol), potassium fluoride (350 mg, 6.0 mmol) and silver (I) nitrate (1 g, 6 mmol) were added in the solution successively. The mixture was heated at 60 °C and stirred overnight. Additional potassium fluoride (350 mg, 6.0 mmol) and silver (I) nitrate (1 g, 6 mmol) were added and then the mixture was stirred for further 12 h. The final mixture was filtered through a Celite column and washed with diethyl ether. The filtrate was washed with water and the organic layer was dried over anhydrous Na_2SO_4 and concentrated under reduced pressure. The crude solid was purified by column chromatography to afford 663 mg of light yellow solid **1** (67%). ^{1}H NMR ($CDCl_3$) δ 6.91 (s, 2H), 2.88-2.84 (t, 4H), 1.64-1.54 (m, 4H), 1.31-1.25 (m, 40H), 0.90-0.86 (t, 6H). FAB-HRMS: Calcd. for $[M+H]^+$: 660.69. Found: 660.20.

Synthesis of Monomer **2** is carried out in a similar procedure as monomer **1** using 2-bromo-3-dodecylsulfothiophene with a yield of 75%. ^{1}H NMR ($CDCl_3$) δ 6.91 (s, 2H), 2.88-2.84 (t, 4H), 1.64-1.54 (m, 4H), 1.30-1.26 (m, 40H), 0.90-0.86 (t, 6H). FAB-HRMS: Calcd. for $[M+H]^+$: 724.82. Found: 724.20.

BiEDOT (3) was prepared according to a modified literature procedure.[25] 3,4-Ethylenedioxythiophene (2 g, 14.0 mmol) was dissolved in anhydrous THF (60 mL). A solution of *n*-BuLi (9.7 ml of 1.6 M solution in hexanes, 15.5 mmol) was added dropwise to the solution at -78 °C. The reaction mixture was stirred for 2 h at 0 °C, followed by addition of $CuCl_2$ in one portion. Then the solution was stirred overnight at the same temperature. The solution was filtered through a Celite column and extracted by CH_2Cl_2. After washed with brine, water and dried over Na_2SO_4, the organic fraction was concentrated in vacuum. The crude product was purified by column chromatography to yield 0.8 g (41%) of **3** as a white solid. ^{1}H NMR ($CDCl_3$) δ 6.27 (s, 2H), 4.34-4.31 (m, 4H), 4.26-4.22 (m, 4H).

Synthesis of polymer PQT12 and PQTS12 is carried out in a similar procedure as in the literature.[26] PDTDE12 and PDTDES12 were firstly synthesized using C-H direct coupling, so we give details of synthetic procedures and characterizations here.

Synthesis of polymer **PDTDE12**

In a 20 mL Schlenk tube with stir bar, a mixture of monomer **1** (105 mg, 0.16 mmol), bisEDOT (45 mg, 0.16 mmol), palladium acetate (0.7 mg, 2 mol%), pivalic acid (5 mg, 0.3 mol%), and potassium carbonate (55 mg, 2.5 eq.) were dissolved in dry *N*, *N*-dimethylacetamide (DMAc) (4 mL). The mixture was flushed and sealed with nitrogen. Then the tube was put into a hot oil bath with a constant temperature of 120 ^{o}C and allowed to stir vigorously for 45 min. A small amount of toluene was added into reaction mixture to dilute the solution and the flask was cooled to room temperature. The mixture was precipitated into methanol and stirred for an hour. The precipitate was purified by using soxhlet extraction thimble and washed successively with methanol, acetone, hexane and finally extracted with the chloroform. After

concentrated under reduced pressure, the solution was precipitated into methanol again. A dark blue solid was obtained in 41% yield (61 mg). M_n = 7.5 kDa, PDI (M_w/M_n) = 1.3, THF as eluent vs. polystyrene standards. Anal. Calcd for $C_{44}H_{62}O_4S_4$: C, 67.56; H, 7.51; O, 9.34; S, 15.59.

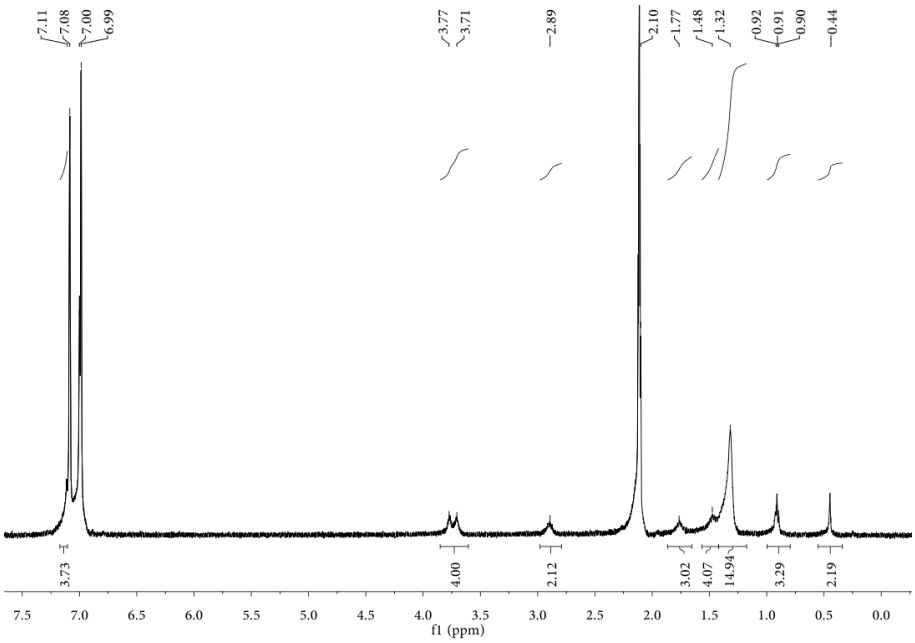

Figure S14. The NMR spectra of PDTDE12 (The data were collected in Toluene-d_8 at 100 ^oC).

Synthesis of polymer **PDTDES12**

This polymer was prepared following the similar procedure for PDTDE12. For PDTDES12, M_n=16.4 kDa, PDI (M_w/M_n) = 1.1, THF as eluent vs. polystyrene standards. Anal. Calcd for $C_{44}H_{62}O_4S_6$: C, 61.35; H, 6.58; O, 10.43; S, 21.64.

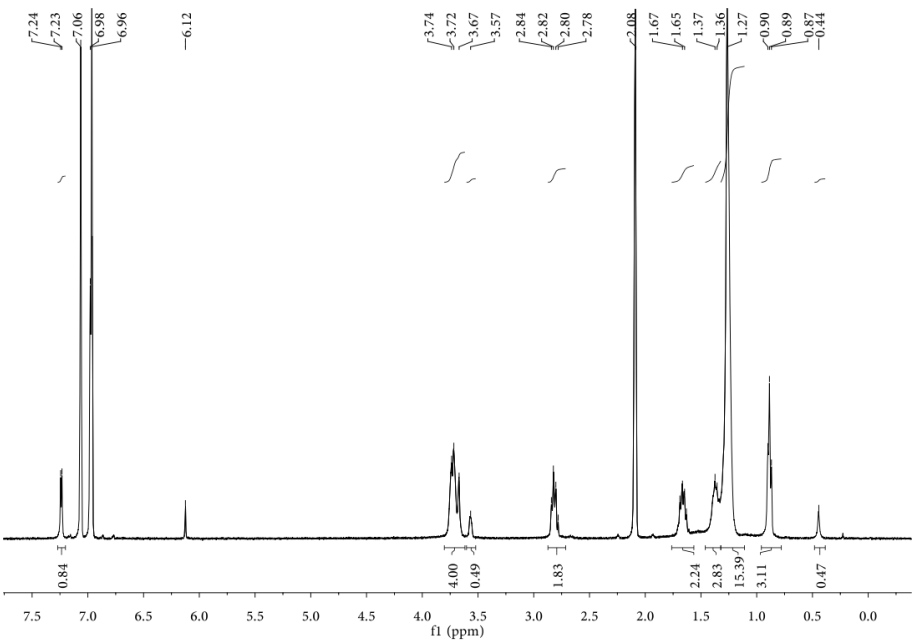

Figure S15. The NMR spectra of PDTDES12 (The data were collected in Toluene-d_8 at 100 ^{o}C).

References:

(1) Chang, W. B.; Fang, H.; Liu, J.; Evans, C. M.; Russ, B.; Popere, B. C.; Patel, S. N.; Chabinyc, M. L.; Segalman, R. A. *ACS Macro Lett.* **2016**, *5*, 455.
(2) Cahill, D. G. *Rev. Sci. Instrum.* **2004**, *75*, 5119.
(3) Hopkins, P. E.; Serrano, J. R.; Phinney, L. M.; Kearney, S. P.; Grasser, T. W.; Harris, C. T. *J. Heat Transfer* **2010**, *132*, 081302.
(4) Schmidt, A. J.; Chen, X.; Chen, G. *Rev. Sci. Instrum.* **2008**, *79*, 114902.
(5) Hopkins, P. E.; Kaehr, B.; Phinney, L. M.; Koehler, T. P.; Grillet, A. M.; Dunphy, D.; Garcia, F.; Brinker, C. J. *J. Heat Transfer* **2011**, *133*, 061601.
(6) Feng, X.; Wang, X. *Thin Solid Films* **2011**, *519*, 5700.
(7) Connelly, N. G.; Geiger, W. E. *Chem. Rev.* **1996**, *96*, 877.
(8) https://en.wikipedia.org/wiki/Nitrosonium
(9) Sonar, P.; Williams, E. L.; Singh, S. P.; Manzhos, S.; Dodabalapur, A. *Phys. Chem. Chem. Phys.* **2013**, *15*, 17064.
(10) Gratia, P.; Magomedov, A.; Malinauskas, T.; Daskeviciene, M.; Abate, A.; Ahmad, S.; Grätzel, M.; Getautis, V.; Nazeeruddin, M. K. *Angew. Chem. Int. Ed.* **2015**, *54*, 11409.
(11) Kim, G. H.; Shao, L.; Zhang, K.; Pipe, K. P. *Nat. Mater.* **2013**, *12*, 719.
(12) Bubnova, O.; Khan, Z. U.; Malti, A.; Braun, S.; Fahlman, M.; Berggren, M.; Crispin, X. *Nat. Mater.* **2011**, *10*, 429.
(13) Aïch, R. B.; Blouin, N.; Bouchard, A.; Leclerc, M. *Chem. Mater.* **2009**, *21*, 751.
(14) Zhang, Q.; Sun, Y.; Xu, W.; Zhu, D. *Energy Environ. Sci.* **2012**, *5*, 9639.
(15) Zhang, Q.; Sun, Y.; Jiao, F.; Zhang, J.; Xu, W.; Zhu, D. *Synth. Met.* **2012**, *162*,

788.
(16) Kang, K.; Watanabe, S.; Broch, K.; Sepe, A.; Brown, A.; Nasrallah, I.; Nikolka, M.; Fei, Z.; Heeney, M.; Matsumoto, D.; Marumoto, K.; Tanaka, H.; Kuroda, S.-i.; Sirringhaus, H. *Nat. Mater.* **2016**, *15*, 896.
(17) Glaudell, A. M.; Cochran, J. E.; Patel, S. N.; Chabinyc, M. L. *Adv. Energy Mater.* **2015**, *5*, 1401072.
(18) Patel, S. N.; Glaudell, A. M.; Kiefer, D.; Chabinyc, M. L. *ACS Macro Lett.* **2016**, *5*, 268.
(19) Cochran, J. E.; Junk, M. J. N.; Glaudell, A. M.; Miller, P. L.; Cowart, J. S.; Toney, M. F.; Hawker, C. J.; Chmelka, B. F.; Chabinyc, M. L. *Macromolecules* **2014**, *47*, 6836.
(20) Duong, D. T.; Wang, C.; Antono, E.; Toney, M. F.; Salleo, A. *Org. Electron.* **2013**, *14*, 1330.
(21) Kroon, R.; Kiefer, D.; Stegerer, D.; Yu, L.; Sommer, M.; Müller, C. *Adv. Mater.* **2017**, 1700930.
(22) Karpov, Y.; Erdmann, T.; Raguzin, I.; Al-Hussein, M.; Binner, M.; Lappan, U.; Stamm, M.; Gerasimov, K. L.; Beryozkina, T.; Bakulev, V.; Anokhin, D. V.; Ivanov, D. A.; Günther, F.; Gemming, S.; Seifert, G.; Voit, B.; Di Pietro, R.; Kiriy, A. *Adv. Mater.* **2016**, *28*, 6003.
(23) Karpov, Y.; Erdmann, T.; Stamm, M.; Lappan, U.; Guskova, O.; Malanin, M.; Raguzin, I.; Beryozkina, T.; Bakulev, V.; Günther, F.; Gemming, S.; Seifert, G.; Hambsch, M.; Mannsfeld, S.; Voit, B.; Kiriy, A. *Macromolecules* **2017**, *50*, 914.
(24) Takahashi, M.; Masui, K.; Sekiguchi, H.; Kobayashi, N.; Mori, A.; Funahashi, M.; Tamaoki, N. *J. Am. Chem. Soc.* **2006**, *128*, 10930.
(25) Hwang, E.; de Silva, K. M. N.; Seevers, C. B.; Li, J.-R.; Garno, J. C.; Nesterov, E. E. *L*angmuir **2008**, *24*, 9700.
(26) Guo, X.; Puniredd, S. R.; Baumgarten, M.; Pisula, W.; Müllen, K. *J. Am. Chem. Soc.* **2012**, *134*, 8404.